

Original Article
Ophthalmology



Assessment of the pigeon (*Columba livia*) retina with spectral domain optical coherence tomography

Sunhyo Kim , Seonmi Kang , Lina Susanti , Kangmoon Seo *

Department of Veterinary Clinical Sciences, College of Veterinary Medicine and Research Institute for Veterinary Science, Seoul National University, Seoul 08826, Korea

 OPEN ACCESS

Received: Mar 23, 2021
Revised: Jul 5, 2021
Accepted: Jul 8, 2021
Published online: Jul 30, 2021

*Corresponding author:

Kangmoon Seo


Department of Veterinary Clinical Sciences,
College of Veterinary Medicine and Research
Institute for Veterinary Science, Seoul National
University, 1 Gwanak-ro, Gwanak-gu, Seoul
08826, Korea.

E-mail: kmseo@snu.ac.kr


© 2021 The Korean Society of Veterinary
Science

This is an Open Access article distributed
under the terms of the Creative Commons
Attribution Non-Commercial License ([https://
creativecommons.org/licenses/by-nc/4.0](https://creativecommons.org/licenses/by-nc/4.0))
which permits unrestricted non-commercial
use, distribution, and reproduction in any
medium, provided the original work is properly
cited.


ORCID iDs

Sunhyo Kim 


<https://orcid.org/0000-0002-3410-8656>

Seonmi Kang 

<https://orcid.org/0000-0001-8017-0891>

Lina Susanti 

<https://orcid.org/0000-0002-6978-0936>

Kangmoon Seo 

<https://orcid.org/0000-0001-6645-7116>

Funding

This study was supported by the BK21 PLUS
Program for Creative Veterinary Science
Research and the Research Institute for
Veterinary Science (RIVS), College of
Veterinary Medicine, Seoul National University,
Seoul 08826, Korea.

<https://vetsci.org>

ABSTRACT

Background: To assess the normal retina of the pigeon eye using spectral domain optical coherence tomography (SD-OCT) and establish a normative reference.

Methods: Twelve eyes of six ophthalmologically normal pigeons (*Columba livia*) were included. SD-OCT images were taken with dilated pupils under sedation. Four meridians, including the fovea, optic disc, red field, and yellow field, were obtained in each eye. The layers, including full thickness (FT), ganglion cell complex (GCC), thickness from the retinal pigmented epithelium to the outer nuclear layer (RPE-ONL), and from the retinal pigmented epithelium to the inner nuclear layer (RPE-INL), were manually measured.

Results: The average FT values were significantly different among the four meridians ($p < 0.05$), with the optic disc meridian being the thickest ($294.0 \pm 13.9 \mu\text{m}$). The average GCC was thickest in the optic disc ($105.3 \pm 27.1 \mu\text{m}$) and thinnest in the fovea meridian ($42.8 \pm 15.3 \mu\text{m}$). The average RPE-INL of the fovea meridian ($165.5 \pm 18.3 \mu\text{m}$) was significantly thicker than that of the other meridians ($p < 0.05$). The average RPE-ONL of the fovea, optic disc, yellow field, and red field were $91.2 \pm 5.2 \mu\text{m}$, $87.7 \pm 5.3 \mu\text{m}$, $87.6 \pm 6.5 \mu\text{m}$, and $91.4 \pm 3.9 \mu\text{m}$, respectively. RPE-INL and RPE-ONL thickness of the red field meridian did not change significantly with measurement location ($p > 0.05$).

Conclusions: Measured data could be used as normative references for diagnosing pigeon retinopathies and further research on avian fundus structure.

Keywords: Fovea; optical coherence tomography; pecten; pigeon; retina

INTRODUCTION

As almost every bird relies heavily on its visual ability to interpret and respond to the environment, visual performance is crucial during its life [1]. Therefore, fundus examination and vision-related research of birds are considered important in avian medicine. Indirect and direct ophthalmoscopes are commonly used for fundus examination, similar to that for other animals. However, these instruments may provide limited diagnostic information and might be inadequate for specific diagnosis of the status of the avian retina [2]. Optical coherence tomography (OCT), a noninvasive imaging technology, has been widely used in veterinary ophthalmology recently [3-6]. As this imaging device provides *in vivo* cross-sections of the

Conflict of Interest

The authors declare no conflicts of interest

Author Contributions

Conceptualization: Kim S, Kang S, Seo K; Data curation: Kim S, Susanti L; Investigation: Kim S, Susanti L; Supervision: Kang S, Seo K; Writing - original draft: Kim S; Writing - review & editing: Kang S, Seo K.

retina with high resolution, it is effectively used for clinical diagnosis and research of various animal eyes, including those of birds [3,7-9].

The basic structures of all vertebrate retinas are similar, but birds have some specific features such as the pecten oculi, a specialized, nutritive structure with an avascular retina, and one or two foveae in their fundus [1]. Although histologic investigations of these avian retinal structures have been performed in several studies [10], the assessment of retinal thickness could be distorted, affecting the ability to reflect the structure of the retina while the animal is alive. Enucleation of the eyes for histopathologic examination is also a clinical limitation. However, OCT has been shown to be helpful in detecting early histologic changes in the retinal layer, changes that are difficult to detect on fundus examination [3,4,6]. Furthermore, OCT scanning is advantageous as it is non-invasive, suitable for serial monitoring, and, unlike histopathologic examination, it reflects distortion-less tissue structure. A few examinations with OCT have been conducted in living birds [3,11-13]; however, no attempt to establish and describe normal OCT data for specific avian species has been made. The purpose of this study was to assess the normal retinal structure of pigeons (*Columba livia*) using OCT images and manual measurements to establish normative references. By establishing the normal reference range for OCT images of pigeon retina and evaluating the retinal structure, the results could contribute to future research on retinal diseases of pigeons and other birds and to visual science-related research. In addition, it is thought that the results would contribute methodologically to active veterinary medicine research establishing reference ranges for normal OCT of companion animals.

MATERIALS AND METHODS

Experimental animals

Twelve eyes of six pigeons (*C. livia*) obtained from a pigeon farm as experimental animals were enrolled in this study. Although their gender was not verified, all birds were adults and over a year old. The mean bodyweight of the pigeons was 278.0 ± 18.3 g (260–310 g). All pigeons were euthanized with intravenous potassium chloride injection under isoflurane anesthesia within one day after OCT scanning.

Ophthalmic examinations and OCT scan

All pigeons were administered 1% rocuronium (Rocunium Inj.; Hana Pharm. Co., Ltd., Korea) topically [14-16] for pupil dilation and sedated with intramuscular medetomidine injection (0.2 mg/kg; Dormitor; Zoetis, USA). Ocular examinations, including slit-lamp biomicroscopy (SL-D7; Topcon Corp., Japan), rebound tonometry (TonoVet; Icare, Tiolat, Finland), and funduscopy (Kowa Hand-held Fundus Camera; Kowa Co., Japan) were conducted.

Following the ophthalmic examinations, spectral domain-OCT (SD-OCT; Optovue; iVue Inc., USA) images were obtained using the system's 'retinal map scan mode' for both the eyes with the sedated pigeons manually restrained by trained veterinarians. During the OCT scan, the head of the pigeons was slightly moved ventrally so the pecten oculi would fall plumb down from the optic disc in the en face image. It helped each OCT image to be taken parallel to a line between two points, the fovea and optic disc (**Fig. 1**). During OCT scanning, the eyes were kept moist with artificial tears (Hyalein Mini 0.3%, Santen Pharm. Co., Ltd., Korea).

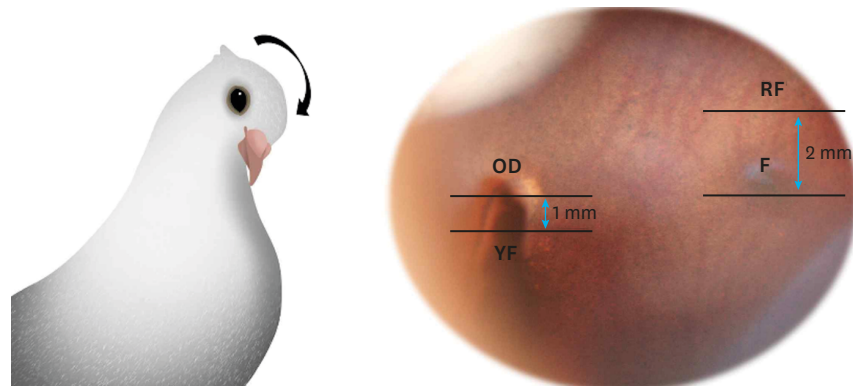


Fig. 1. Schematic image of a pigeon and a fundoscopic image. The pigeon was restrained with the head slightly moved ventrally (see arrow direction). Four meridians are presented on the fundoscopic image. OD, optic disc; F, fovea; YF, yellow field; RF, red field.

Measurement

In this study, pigeon retina dimensions were demonstrated in four meridians in cut sections of the tissue from which the tomographic images were taken. The meridians included the fovea, optic disc, red field, and yellow field. Although the pigeon has a variable and less well-differentiated fovea [10], it can be easily detected on the nasal region from the optic disc. The red field of the retina, known as the area dorsalis of the pigeon, is one of the two major regions for vision with the fovea. A high density of red oil droplets is present in the cone cells in this area and in the superior dorsal quadrant [10]. In this study, a meridian located 2 mm dorsally from the fovea represented the red field. The remainder of the pigeon retina, called the yellow field, was represented by a meridian located 1 mm ventrally from the optic disc. The fovea and optic disc images were taken at the center of the meridian (**Fig. 1**).

Each eye was evaluated in the four areas (fovea, optic disc, yellow field, and red field) by applying the retina map scan mode, which was generally used to analyze the fovea and macular volume. It provides 20 horizontal cross-sections of the 6×6 mm retinal field and the average thickness via an early treatment diabetic retinopathy study (ETDRS) grid. As the center of the ETDRS grid could be moved to the desired position, it helped when choosing the meridian, which was placed some distance from objective points, such as the fovea and optic disc, prior to taking the measurements. The thickness of the layers was manually measured at five locations (0 mm, ± 1 mm, ± 2 mm) relative to the center of each meridian. Nasal and temporal directions were marked + and -, respectively, with the "0 mm" region defined as the center and each point measured every millimeter from the center toward the periphery. Four layers including full thickness (FT; from the retinal pigmented epithelium [RPE] to the inner limiting membrane), thickness of the ganglion cell complex (GCC; from the inner limiting membrane to the ganglion cell layer [GCL]), thickness of photoreceptor minus its axon (RPE-ONL; from RPE to outer nuclear layer), and thickness from the RPE to the inner nuclear layer (RPE-INL) were measured in all meridians. Only high-quality images were chosen, and the data were measured using the software included with the OCT device.

Histological examination

To identify the histological structure of the pigeon retina and compare findings with those of OCT images, one enucleated globe was fixed with formalin and stained with hematoxylin and eosin.

Statistical analyses

All statistical analyses were performed using commercial statistical software (R version 3.4.1). For describing statistical data, means, SD, and confidence intervals of 95% were used. A one-way analysis of variance (ANOVA) test was used to compare differences in layer thickness according to measurement locations from the - 2 mm to + 2 mm region within each meridian. The average thicknesses of each layer in each meridian were compared using a one-way ANOVA test. Pairwise comparisons across the locations were adjusted for multiple comparisons using the post hoc Tukey test in all four meridians.

Ethical approval statement

All procedures were performed with the approval of the Institutional Animal Care and Use Committee. This study was approved by the Seoul National University Institutional Animal Care and Use Committee (IACUC, SNU-191002-5)

RESULTS

Ophthalmic examination

There was no abnormality in all of the pigeon eyes examined under slit-lamp biomicroscopy or funduscopy. The mean intraocular pressure (IOP) was 11.7 ± 1.7 mm Hg.

Histological evaluation

Histological segmentation of the pigeon retina is shown in (Fig. 2), and all retinal layers could be observed. The nerve fiber layer (NFL) was thicker near the pecten, and the NFL thickness varied markedly depending on location. The GCL consisted of about 1–3 nuclear layers and appeared thicker near the fovea. The INL and ONL consisted of approximately 9–20 and 2–4 nuclear layers, respectively. The IPL and INL occupied more than 50% of the whole retinal thickness. The outer plexiform layer (OPL) appeared to be not very developed. At most locations, the RPE and the photoreceptor layer were separated during the slide production process.

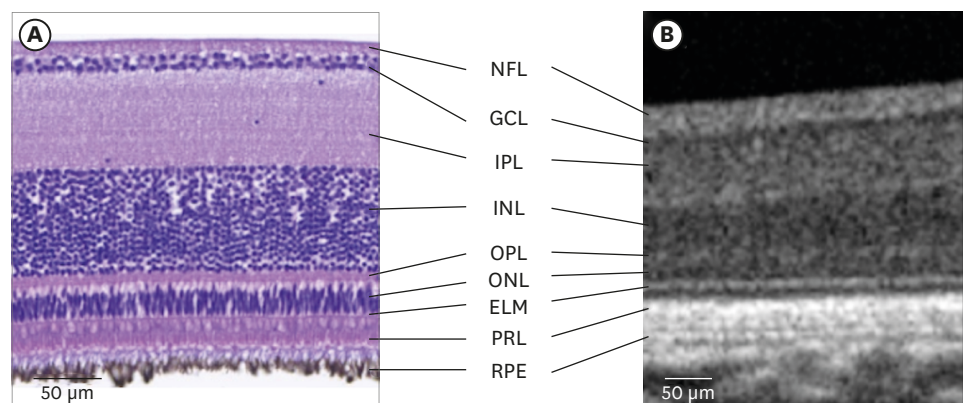


Fig. 2. Histologic segmentation of the pigeon retina (A) and a corresponding image obtained with an optical coherence tomography device (B).

NFL, nerve fiber layer; GCL, ganglion cell layer; IPL, inner plexiform layer; INL, inner nuclear layer; OPL, outer plexiform layer; ONL, outer nuclear layer; ELM, external limiting membrane; PRL, photoreceptor layer; RPE, retinal pigmented epithelium.

The SD-OCT images

All retinal layers could be identified and are presented in **Fig. 2**. The four meridians, including the fovea, optic disc, yellow field, and red field, were determined and are presented in **Figs. 3, 4, and 5**. Because OCT did not permit visualization of the structure under the pecten, the OCT images included shadows in the middle of the optic disc and yellow field meridians.

Full thickness (FT)

The FTs of the pigeon retinas in all meridians are presented in **Table 1**. The average FT of the fovea meridian was $275.3 \pm 11.2 \mu\text{m}$. The fovea was noticeable as a small pit about 1 mm in diameter nasally from the optic disc. Although there was slight variation depending on the location, the 2 mm region was significantly thinner than the other regions in this meridian. The average FT of the optic disc and yellow field meridians were $294.0 \pm 13.9 \mu\text{m}$ and $284.3 \pm 10.2 \mu\text{m}$, respectively. The FT of the “+ 1 mm” and “- 1 mm” regions were significantly greater than those of the “+ 2 mm” and “- 2 mm” regions ($p < 0.05$), and these meridians were symmetrical about the pecten. The average FT of the red field meridian was $261.1 \pm 6.6 \mu\text{m}$, the thinnest among the measured meridians.

Ganglion cell complex (GCC) thickness

The GCC thicknesses of the pigeon retinas in all meridians are presented in **Table 2**. The average GCC thickness of the fovea meridian was $42.8 \pm 15.3 \mu\text{m}$. GCC of the fovea (0 mm)

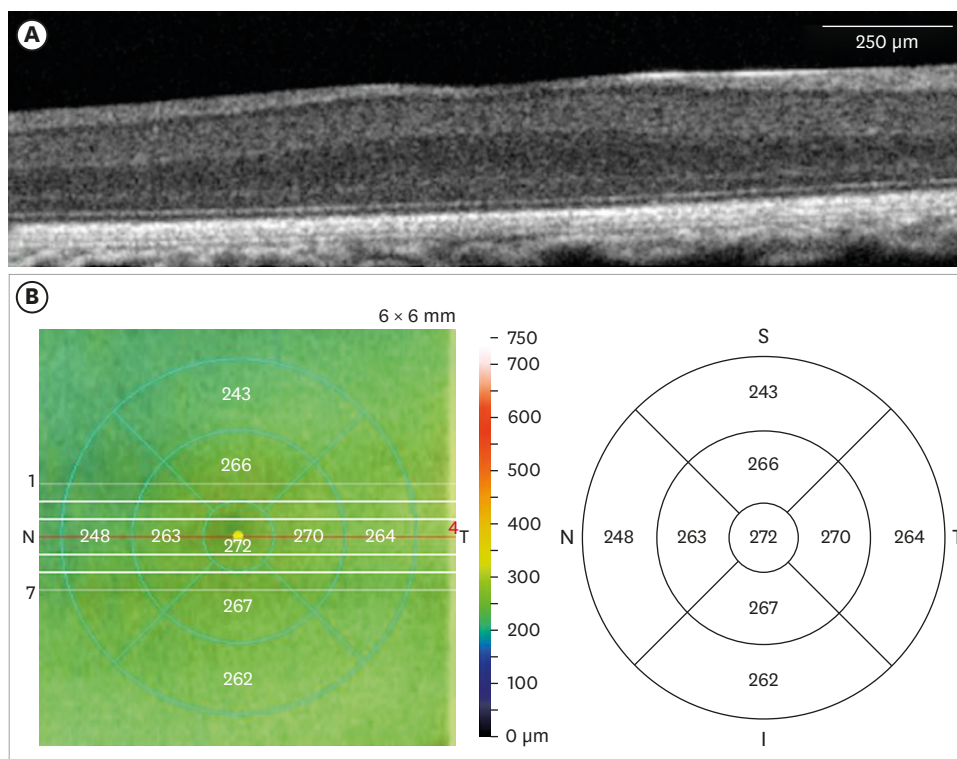


Fig. 3. Retina map based on OCT scanning of the pigeon left eye. (A) Tomographic image of the fovea meridian. The fovea is seen as a small pit at the center of the image. A scale bar is present. (B) NDB reference map with the ETDRS grid and associated values on the right circle. The ETDRS grid was positioned on the center of the fovea. The color scale of the NDB reference represents normative data in humans. The red line corresponds to the fovea meridian, which is shown in (A). S, superior; T, temporal; I, inferior; N, nasal; OCT, optical coherence tomography; NDB, normal database; ETDRS, early treatment diabetic retinopathy study.

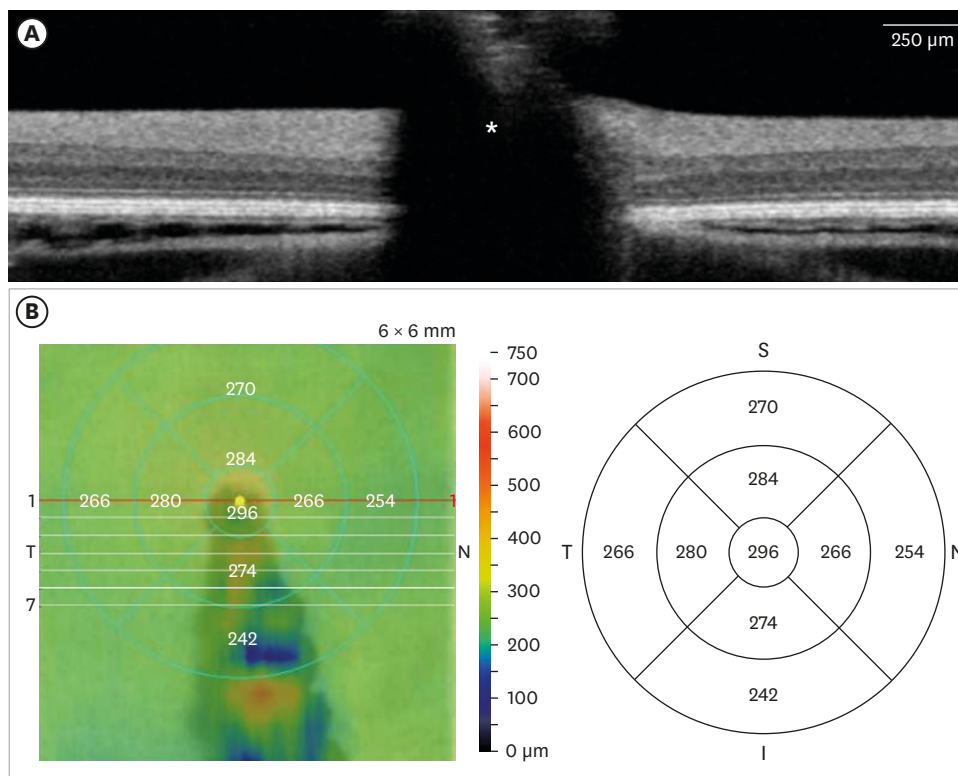


Fig. 4. Retina map OCT scan of the pigeon optic disc. (A) Tomographic image of the optic disc meridian. The structure under the pecten (*) was not visualized on the OCT image. A scale bar is present. (B) NDB reference map with the ETDRS grid and associated values on the right circle. The ETDRS grid was positioned at the center of the optic disc where the pecten originated. The color scale of the NDB reference represents normative data in humans. The red line corresponds to the optic disc meridian, which is shown in (A). S, superior; T, temporal; I, inferior; N, nasal; OCT, optical coherence tomography; NDB, normal database; ETDRS, early treatment diabetic retinopathy study.

was significantly thinner than that of the other regions within this meridian ($p < 0.05$). The retinal ganglion cell layer of the fovea was thicker than the peri-foveal region, but the nerve

Table 1. Measured pigeon retinal full thickness (µm) in four meridian locations

Location	Temporal				Nasal		Average
	-2 mm	-1 mm	0 mm	+1 mm	+2 mm		
Fovea	278.3 ± 5.2 ^{b,*}	283.8 ± 7.3 ^b	279.0 ± 5.8 ^b	278.0 ± 7.5 ^b	257.3 ± 5.9 ^a	275.3 ± 11.2 ^b	
Optic disc	287.9 ± 8.0 ^a	310.7 ± 6.8 ^c	-	296.9 ± 9.8 ^b	280.3 ± 8.0 ^a	294.0 ± 13.9 ^d	
Yellow field	280.4 ± 6.4 ^{a,b}	293.8 ± 8.4 ^c	-	287.4 ± 9.3 ^{b,c}	275.3 ± 6.0 ^a	284.3 ± 10.2 ^c	
Red field	266.3 ± 8.4 ^c	263.0 ± 5.5 ^{b,c}	258.9 ± 5.4 ^{a,b}	255.9 ± 3.7 ^a	261.3 ± 4.3 ^{a,c}	261.1 ± 6.6 ^a	

At the center of optic disc and yellow field meridians, measuring was not possible due to the presence of the pecten.

*Mean ± SD.

^{a,b,c}Different superscript letters mean significant differences in the same meridian and average column, respectively ($p < 0.05$).

Table 2. Measured pigeon retinal ganglion cell complex thickness (µm) in four meridian locations

Location	Temporal				Nasal		Average
	-2 mm	-1 mm	0 mm	+1 mm	+2 mm		
Fovea	60.0 ± 10.4 ^c	37.6 ± 10.7 ^b	25.3 ± 6.8 ^a	42.7 ± 14.0 ^b	48.3 ± 8.5 ^{b,c}	42.8 ± 15.3 ^a	
Optic disc	98.8 ± 9.8 ^{a,b}	135.9 ± 9.3 ^c	-	107.3 ± 10.8 ^b	79.3 ± 32.0 ^a	105.3 ± 27.1 ^c	
Yellow field	93.0 ± 7.2 ^b	121.7 ± 16.6 ^c	-	99.3 ± 13.7 ^b	69.1 ± 9.5 ^a	95.8 ± 22.4 ^c	
Red field	64.6 ± 8.0 ^c	59.3 ± 6.0 ^{b,c}	52.9 ± 6.3 ^{a,b}	50.9 ± 4.4 ^a	58.7 ± 6.0 ^{b,c}	57.3 ± 7.8 ^b	

At the center of optic disc and yellow field meridians, measuring was not possible due to the presence of the pecten.

*Mean ± SD.

^{a,b,c}Different superscript letters mean significant differences in the same meridian and average column, respectively ($p < 0.05$).

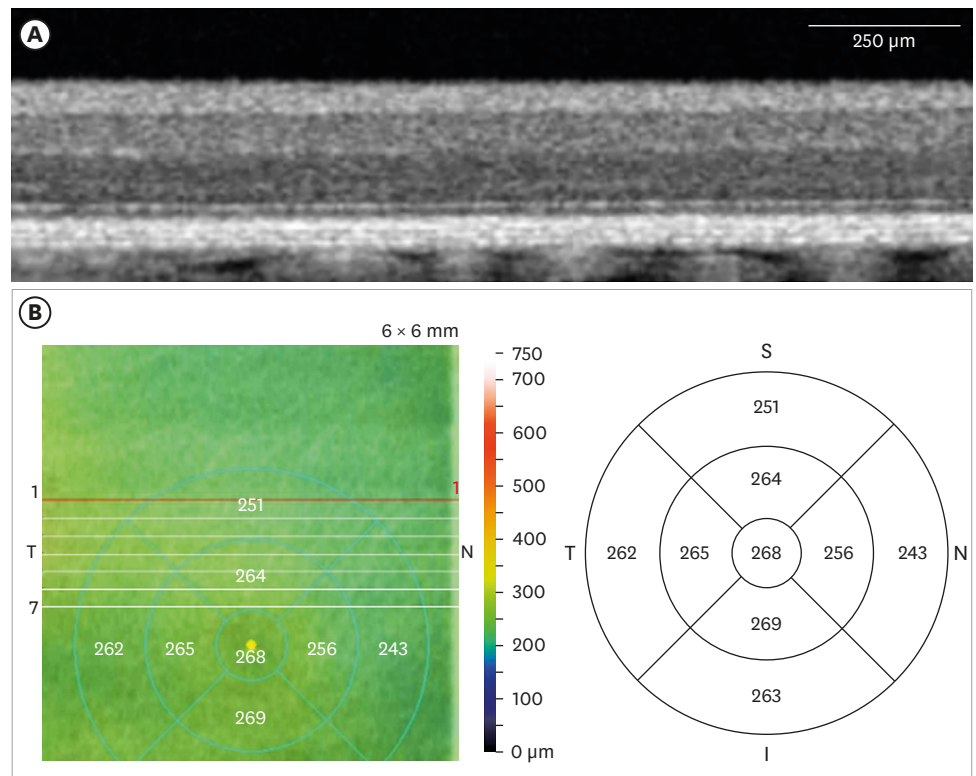


Fig. 5. Retina map optical coherence tomography scan of the pigeon optic disc. (A) Tomographic image of the red field meridian. A scale bar is present. (B) NDB reference map with the ETDRS grid and associated values on the right circle. The ETDRS grid was positioned at the center of the fovea. The color scale of the NDB reference represents normative data in humans. The red line corresponds to the red field meridian, shown in (A), and is located 2 mm dorsally from the fovea. S, superior; T, temporal; I, inferior; N, nasal; NDB, normal database; ETDRS, early treatment diabetic retinopathy study.

fiber layer was thinner than the other regions. The average GCC thicknesses of the optic disc and yellow field meridian were $105.3 \pm 27.1 \mu\text{m}$ and $95.8 \pm 22.4 \mu\text{m}$, respectively. GCC of the ± 1 mm region of these meridians was significantly thicker than the ± 2 mm region ($p < 0.05$), indicating that the closer to the pecten, the thicker the GCC. The average GCC thickness of the red field meridian was $57.3 \pm 7.8 \mu\text{m}$.

Retinal pigmented epithelium to inner nuclear layer (RPE-INL) thickness

The RPE-INL thicknesses of the pigeon retinas in all meridians are presented in **Table 3**. The average RPE-INL thickness was the thickest in the fovea meridian, and it was $165.5 \pm 18.3 \mu\text{m}$ ($p < 0.05$). At the fovea, which is the central region of this meridian (0 mm), the RPE-INL thickness was significantly thicker than that in other regions ($p < 0.05$). The average RPE-INL thickness of the optic disc and yellow field meridians were $138.7 \pm 10.2 \mu\text{m}$ and 136.8 ± 10.9

Table 3. Measured retinal pigmented epithelium to the inner nuclear layer thickness (μm) of the pigeon retina in four meridian locations

Location	Temporal		0 mm	Nasal		Average
	-2 mm	-1 mm		+1 mm	+2 mm	
Fovea	151.7 ± 5.6^a	169.8 ± 7.2^b	195.3 ± 8.9^c	162.7 ± 8.9^b	148.0 ± 3.9^a	165.5 ± 18.3^c
Optic disc	137.8 ± 5.8^b	128.4 ± 8.6^a	-	138.5 ± 7.6^b	150.0 ± 5.2^c	138.7 ± 10.2^a
Yellow field	135.8 ± 6.6^b	125.1 ± 9.1^a	-	139.6 ± 8.0^b	146.6 ± 7.1^c	136.8 ± 10.9^a
Red field	144.9 ± 3.4	146.3 ± 2.9	147.7 ± 3.3	146.3 ± 2.9	145.0 ± 2.7	146.1 ± 3.1^b

At the center of optic disc and yellow field meridians, measuring was not possible due to the presence of the pecten.

*Mean \pm SD.

^{a,b,c}Different superscript letters mean significant differences in the same meridian and average column, respectively ($p < 0.05$).

Table 4. Measured retinal pigmented epithelium to the outer nuclear layer thickness (μm) of the pigeon retina in four meridian locations

Location	Temporal			Nasal		Average
	-2 mm	-1 mm	0 mm	+1 mm	+2 mm	
Fovea	90.6 \pm 4.6	92.3 \pm 5.4	93.7 \pm 5.5	88.5 \pm 5.5	91.0 \pm 3.9	91.2 \pm 5.2 ^b
Optic disc	87.7 \pm 4.0 ^{a,b}	84.8 \pm 5.3 ^a	-	87.6 \pm 5.9 ^{a,b}	90.7 \pm 4.7 ^b	87.7 \pm 5.3 ^a
Yellow field	87.8 \pm 5.0 ^{a,b}	82.3 \pm 6.8 ^a	-	88.4 \pm 6.6 ^{a,b}	92.0 \pm 3.6 ^b	87.6 \pm 6.5 ^a
Red field	90.7 \pm 4.1	91.3 \pm 3.1	92.0 \pm 3.6	91.3 \pm 5.1	91.7 \pm 3.6	91.4 \pm 3.9 ^b

At the center of optic disc and yellow field meridians, measuring was not possible due to the presence of the pecten.

*Mean \pm SD.

^{a,b,c}Different superscript letters mean significant differences in the same meridian and average column, respectively ($p < 0.05$).

μm , respectively, and they were not significantly different. In the ± 1 mm region, RPE-INL was significantly thinner than that in the ± 2 mm region in these meridians. The average RPE-INL thickness of the red field meridian was $146.1 \pm 3.1 \mu\text{m}$. The RPE-INL of this meridian showed no significant difference in thickness depending on the measured location.

Retinal pigmented epithelium to outer nuclear layer (RPE-ONL) thickness

The RPE-ONL thicknesses of the pigeon retinas in all meridians are presented in **Table 4**. The average RPE-ONL thickness of the fovea and red field meridians were $91.2 \pm 5.2 \mu\text{m}$ and $91.4 \pm 3.9 \mu\text{m}$, respectively, and were not significantly different. There was no significant difference in RPE-ONL thickness depending on location in the fovea or red field meridians. The average RPE-ONL thicknesses of the optic disc and yellow field meridians were $87.7 \pm 5.3 \mu\text{m}$ and $87.6 \pm 6.5 \mu\text{m}$, respectively, and were not significantly different.

DISCUSSION

Pigeons used in this study were all ophthalmologically normal. However, the exact range for normal IOP in pigeons has not been established. A few researchers have measured pigeon IOP, and they reported a normal IOP range of 5.42 ± 2.06 mm Hg to 19.5 ± 4.4 mm Hg [17,18].

As in previous papers, in this study, OCT was used to obtain tomographic images of living tissues. Conventional examination of the retinal structure in birds has relied on histopathology, which was inevitable for enucleation. Furthermore, histopathological examination could include artifacts, especially when measuring the thickness of the NFL, related to tissue swelling, autolysis, shrinkage, and inadvertent oblique sectioning [19]. In this study, not only NFL but also the other retinal layers were evaluated reliably using OCT images. Compared with the histologic evaluation, the tomographic images obtained via OCT are considered to show the retinal layer structure well. Moreover, distortion of retinal structure, which was observed in the histological specimens, was not seen in the OCT images.

In a previous paper, the dorsal field of the pigeon retina was defined as the red field, and this area showed no macroscopic differences, other than red oil droplets in its photoreceptors, from the surrounding peripheral retinal area (yellow field) [10]. The meridians were defined in this study to represent the red and yellow field of pigeon retina and two other specific structures: fovea and optic disc. In this study, to assess the structure of the pigeon retina using OCT, these four meridians were compared by assessing measurements of retinal layer thicknesses in each meridian.

Previous OCT studies in various animals have provided valuable information for estimating the normal structure of the pigeon retina [2,7,20]. In this study, we observed all of the retinal

layers in the OCT images of pigeons that had previously been observed in other vertebrates. However, the OPL was thin, and its boundaries were unclear in all meridians, indicating that the outer border of the INL and the inner border of the ONL might be inaccurately assessed. For this reason, the distance from the outer border of the RPE to the inner border of the INL was measured to provide an estimate for the INL. Andrew et al. [20] reported that the OPL of the pigeon retina was a tri-stratified structure because the photoreceptors end at three different levels. This type of stratification arranges the dendrites of the bipolar and horizontal cells in a lamellar structure, and the unclear boundaries of the OPL might reflect this anatomical characteristic. The unclear inner boundary of the ONL limited measurement of the thickness of the photoreceptor cells; thus, the distance from the outer border of the RPE to the inner border of the ONL was measured in this study. OPL was not included in photoreceptor thickness as it was previously shown to be dependent on the neurons of the bipolar and horizontal cells [4].

The fovea, one of the distinguishing structures of birds, is an area for high visual acuity that differs among species [20]. The fovea of the pigeon retina in this study was observed to be a shallow saucer-shaped depression of the anthropoid type. This type of fovea can be present in primates and in the temporal fovea of some bifoveate birds [21]. The other type of fovea, known as the convexiculate, is deep and funnel- or whirlpool-shaped and is commonly present in fish, reptiles, and birds [21]. The anthropoid-type fovea in the pigeon retina in this study had a statistically insignificant FT compared to the thickness in the peri-fovea region, contrary to that of the convexiculate fovea, which, as reported previously, has a notably decreased FT at the fovea due to the absence of all retinal layers proximal to the ONL [6]. The relationship between the shape of the fovea and its function remains incompletely described [22].

The fovea and red field are high visual acuity regions in the pigeon retina and have similar mean visual acuity when measured behaviorally [10,23,24]. It has been reported that pigeons have a 350–400 μm diameter rod-free region at the center of the fovea, colocalizing with the area of highest cone cell density in the photoreceptor layer [10]. Likewise, the red field has 1.3–3 times higher cone cell density than that of the yellow field [10]. Single cone cell synapses with single bipolar cells are associated with a higher visual resolution, whereas several rods converge upon a single bipolar cell [25]. For these reasons, the INL, which represents bipolar cell bodies, may be thick at the fovea and in the red field meridian. In this study, the RPE-INL of the fovea and red field meridian were significantly thicker than those of the optic disc and the yellow field meridian. In the cone-rich retinas of most domestic animals, the number of bipolar cells is remarkably high and similar to amacrine cell density [8]. As the rod cell density of the pigeon retina is invariable in all retinal fields, except the rod-free region at the center of the fovea [10], the differences in cone cell density seem to be reflected in the pigeon INL thickness.

When comparing the thicknesses of the pigeon retinal layers, including FT, GCC, and RPE-INL, the location of the measurement was critical, as significant differences were detected depending on the meridian (**Tables 1, 2, and 3**). In particular, the GCC thickness was highly variable and affected the FT values in this study. For this reason, comparing only FT might be effective in some diseases that primarily affect the GCC, such as glaucoma, but might be less sensitive to retinopathies that first affect photoreceptors. Unlike FT, the absolute differences among the meridians in the average RPE-ONL thickness were insignificant, although the fovea and red field meridians were statistically thicker than the optic disc and yellow field meridians (**Table 4**). This suggests that the pigeon retina has a comparatively uniform photoreceptor cell body layer thickness, regardless of rod and cone densities.

As it was difficult to measure accurately the GCL alone in the pigeon retina, its measurement was done representatively in this study. Unlike other regions, the GCL of the fovea was thick enough to be realized in the foveal meridian. This tendency was similar to a previous histopathological report that showed the ganglion cell density of the fovea was higher than those in other regions [10]. A high pigeon cone cell density was also observed in the fovea. The convergence of the cone cell to ganglion cell ratio was reported to be 2.1 in the fovea and > 4.6 in the other fields [10]. This could be the reason for the GCL of the red field meridian to be less remarkable than that of the fovea.

One of the main purposes of this study was to establish a normative reference of normal pigeon retinal thickness by using OCT, as such imaging information could be used in the diagnosis of pigeon retinopathies and be helpful in further studies on avian fundus structure. Many retinal disorders are known to affect specific retinal layer components primarily. Although the cellular composition of each meridian is different, the red field meridian was considered the ideal region in which to establish a normative reference index for future screening purposes. This meridian was a region with high visual cell density and the least variation in RPE-ONL and RPE-INL thickness depending on the measurement location (Tables 3 and 4). If the thickness of retinal layers changes markedly depending on the measured location in some meridians, the measurement might be inadequate as a reference as it could be easily altered with each measurement. Evaluating GCC thickness and its structure could be advantageous in assessing the fovea meridian. To confirm such suggestions, an additional study comparing affected and normal pigeons should be conducted.

The small number and the confined age of the study pigeons are considered the most significant limitations of this study. It was reported that the number and the acuity of photoreceptors of pigeons decrease with age [26]. All pigeons in this study were over one year old. As suggested in a previous report that generated baseline OCT measurements for other species retinas, multiple groups categorized by age could be included in further research [4]. Despite these limitations, this study provides a valuable initial index of pigeon retinal characteristics. The results could be helpful in future studies into various retinal diseases of pigeons or when establishing normative indices for other species.

Tomographic images of the living pigeon retina were obtained using SD-OCT in this study. The measured values could provide the normative SD-OCT references for use in the diagnosis of pigeon retinopathies and in further research on avian fundus structure. Furthermore, it is considered that the methodology used in this study could be applied to other species when establishing normative SD-OCT references for animal retinas.

REFERENCES

1. Jones MP, Pierce KE Jr, Ward D. Avian vision: a review of form and function with special consideration to birds of prey. *J Exot Pet Med.* 2007;16(2):69-87.
[CROSSREF](#)
2. Azmanis P, Rauscher FG, Werner B. The additional diagnostic value of optical coherence tomography (OCT) and its application procedure in a wide variety of avian Species. *J Clin Exp Ophthalmol.* 2015;6(03):431.
[CROSSREF](#)
3. Rauscher FG, Azmanis P, Körber N, Koch C, Hübel J, Vetterlein W, et al. Optical coherence tomography as a diagnostic tool for retinal pathologies in avian ophthalmology. *Invest Ophthalmol Vis Sci.* 2013;54(13):8259-8269.
[PUBMED](#) | [CROSSREF](#)

4. Ofri R, Ekesten B. Baseline retinal OCT measurements in normal female beagles: the effects of eccentricity, meridian, and age on retinal layer thickness. *Vet Ophthalmol.* 2020;23(1):52-60.
[PUBMED](#) | [CROSSREF](#)
5. Famose F. Assessment of the use of spectral domain optical coherence tomography (SD-OCT) for evaluation of the healthy and pathological cornea in dogs and cats. *Vet Ophthalmol.* 2014;17(1):12-22.
[PUBMED](#) | [CROSSREF](#)
6. Espinheira Gomes F, Abou-Madi N, Ledbetter EC, McArt J. Spectral-domain optical coherence tomography imaging of normal foveae: A pilot study in 17 diurnal birds of prey. *Vet Ophthalmol.* 2020;23(2):347-357.
[PUBMED](#) | [CROSSREF](#)
7. McLellan GJ, Rasmussen CA. Optical coherence tomography for the evaluation of retinal and optic nerve morphology in animal subjects: practical considerations. *Vet Ophthalmol.* 2012;15 Suppl 2:13-28.
[PUBMED](#) | [CROSSREF](#)
8. Gelatt KN, Gilger BC, Kern TJ. Chapter 2. Ophthalmic anatomy. In: Samuelson DA, editor. *Veterinary Ophthalmology*, 5th ed. Ames: Wiley-Blackwell; 2013, 39-668.
9. Rosolen SG, Rivière ML, Lavillegrand S, Gautier B, Picaud S, LeGargasson JF. Use of a combined slit-lamp SD-OCT to obtain anterior and posterior segment images in selected animal species. *Vet Ophthalmol.* 2012;15 Suppl 2:105-115.
[PUBMED](#) | [CROSSREF](#)
10. Querubin A, Lee HR, Provis JM, O'Brien KM. Photoreceptor and ganglion cell topographies correlate with information convergence and high acuity regions in the adult pigeon (*Columba livia*) retina. *J Comp Neurol.* 2009;517(5):711-722.
[PUBMED](#) | [CROSSREF](#)
11. Huang Y, Cideciyan AV, Papastergiou GI, Banin E, Semple-Rowland SL, Milam AH, et al. Relation of optical coherence tomography to microanatomy in normal and rd chickens. *Invest Ophthalmol Vis Sci.* 1998;39(12):2405-2416.
[PUBMED](#)
12. Moayed AA, Hariri S, Song ES, Choh V, Bizheva K. *In vivo* volumetric imaging of chicken retina with ultrahigh-resolution spectral domain optical coherence tomography. *Biomed Opt Express.* 2011;2(5):1268-1274.
[PUBMED](#) | [CROSSREF](#)
13. Ruggeri M, Major JC Jr, McKeown C, Knighton RW, Puliafito CA, Jiao S. Retinal structure of birds of prey revealed by ultra-high resolution spectral-domain optical coherence tomography. *Invest Ophthalmol Vis Sci.* 2010;51(11):5789-5795.
[PUBMED](#) | [CROSSREF](#)
14. Baine K, Hendrix DV, Kuhn SE, Souza MJ, Jones MP. The efficacy and safety of topical rocuronium bromide to induce bilateral mydriasis in hispaniolan amazon parrots (*Amazona ventralis*). *J Avian Med Surg.* 2016;30(1):8-13.
[PUBMED](#) | [CROSSREF](#)
15. Petritz OA, Guzman DS, Gustavsen K, Wiggans KT, Kass PH, Houck E, et al. Evaluation of the mydriatic effects of topical administration of rocuronium bromide in Hispaniolan Amazon parrots (*Amazona ventralis*). *J Am Vet Med Assoc.* 2016;248(1):67-71.
[PUBMED](#) | [CROSSREF](#)
16. Barsotti G, Briganti A, Spratte JR, Ceccherelli R, Breggi G. Mydriatic effect of topically applied rocuronium bromide in tawny owls (*Strix aluco*): comparison between two protocols. *Vet Ophthalmol.* 2010;13 Suppl:9-13.
[PUBMED](#) | [CROSSREF](#)
17. Lim J, Kang S, Park S, Park E, Nam T, Jeong S, et al. Intraocular pressure measurement by rebound tonometry (tonovet) in normal pigeons (*Columba livia*). *J Avian Med Surg.* 2019;33(1):46-52.
[PUBMED](#) | [CROSSREF](#)
18. Karimi V, Asadi F, Rajaei SM, Golabdar S. Intraocular pressure measurements using rebound tonometry in eight different species of companion birds. *J Avian Med Surg.* 2020;34(4):338-342.
[PUBMED](#) | [CROSSREF](#)
19. Frenkel S, Morgan JE, Blumenthal EZ. Histological measurement of retinal nerve fibre layer thickness. *Eye (Lond).* 2005;19(5):491-498.
[PUBMED](#) | [CROSSREF](#)
20. Mariani AP. Neuronal and synaptic organization of the outer plexiform layer of the pigeon retina. *Am J Anat.* 1987;179(1):25-39.
[PUBMED](#) | [CROSSREF](#)
21. Pumphrey RJ. The theory of the fovea. *J Exp Biol.* 1948;25(3):299-312.
[CROSSREF](#)

22. Bringmann A. Structure and function of the bird fovea. *Anat Histol Embryol.* 2019;48(3):177-200.
[PUBMED](#) | [CROSSREF](#)
23. Hodos W, Bessette BB, Macko KA, Weiss SR. Normative data for pigeon vision. *Vision Res.* 1985;25(10):1525-1527.
[PUBMED](#) | [CROSSREF](#)
24. Hodos W, Miller RF, Fite KV. Age-dependent changes in visual acuity and retinal morphology in pigeons. *Vision Res.* 1991;31(4):669-677.
[PUBMED](#) | [CROSSREF](#)
25. Maggs DJ, Miller PE, Ofri R. *Slatter's Fundamentals of Veterinary Ophthalmology.* 6th ed. St. Louis: Elsevier Inc.; 2018, 347-398.
26. Fitzgerald ME, Tolley E, Frase S, Zagvazdin Y, Miller RF, Hodos W, et al. Functional and morphological assessment of age-related changes in the choroid and outer retina in pigeons. *Vis Neurosci.* 2001;18(2):299-317.
[PUBMED](#) | [CROSSREF](#)